Japanese Jadeite: History, Characteristics, and Comparison with Other Sources

Ahmadjan Abduriyim, Kazuko Saruwatari, and Yusuke Katsurada

Even though Japanese jadeite lacks the transparency of the highest-quality Burmese imperial jadeite, its rarity and natural features make it a highly valued gemstone. In this study, jadeite from the Itoigawa and Omi regions in Niigata Prefecture and the Wakasa region in Tottori Prefecture, both on Japan's western coast, were divided into several color varieties corresponding to chromophores and mineral phases: white (nearly pure jadeite), green (Fe-rich, Cr-bearing), lavender (Ti-bearing), blue (Ti- and Fe-bearing), and black (graphite-bearing). White jadeite from Itoigawa-Omi was close to pure jadeite (X_{Jd} = 98, or 98% jadeite composition). Green jadeite from the same location had an X_{Jd} range from 98 to 82. The maximum CaO content in green jadeite was 5 wt.%, and its chromophores were Fe and Cr. Whereas lavender samples had a jadeite composition of X_{Jd} = 98 to 93 and tended to be high in TiO_2 and FeO_{tot} and low in MnO content, blue jadeite showed the highest TiO_2 concentration at 0.65 wt.% and had an X_{Jd} range of 97 to 93. A blue jadeite from Wakasa had a range of 97 to 91 and a similarly high TiO_2 concentration. In trace-element analysis, chondrite-normalized and primitive mantle–normalized patterns in lavender, violetish blue, and blue jadeite from Japan showed higher large-ion lithophile element contents (Sr, Ba) and higher field strength element contents (Zr, Nb) than those in green jadeite, while white and black jadeite had relatively low REE contents. The Japanese jadeites were compared to samples from Myanmar, Guatemala, and Russia.

Japan is an important source of jadeite, much of which comes from the Itoigawa and Omi regions in Niigata Prefecture. The Kotaki area upstream of the Hime River in Itoigawa-Omi was the first documented source of gem-quality jadeite and jadeite-bearing rocks in Japan (Kawano, 1939; Ohmori, 1939). This area is located in the high-pressure, low-temperature metamorphic Renge belt within a Late Paleozoic subduction zone (Shibata and Nozawa, 1968; Nishimura, 1998). Tsujimori (2002) suggested that blueschist to eclogite metamorphism was related to the subduction of oceanic crust. Miyajima et al. (1999, 2001, 2002) and Morishita (2005) proposed that the fluids that facilitated the formation of jadeite in Itoigawa-Omi were related to subduction zones. U-Pb zircon dating of jadeite-natrolite rocks in the area indicated that the age of jadeitization is about 519±17 Ma (Kunugiza et al., 2002; Tsutsumi et al., 2010).

This study introduces the historical background and sources of Japanese jadeite (figure 1). It describes

Figure 1. A large, attractive jadeite boulder from Itoigawa, Japan, characterized by mixed white and green colors. This boulder weighs 40.5 kg and measures approximately 39 cm high, 32 cm long, and 26 cm wide. Photo by Ahmadjan Abduriyim.

See end of article for About the Authors and Acknowledgments.
Gems & Gemology, Vol. 53, No. 1, pp. 48–67,
http://dx.doi.org/10.5741/GEMS.53.1.48

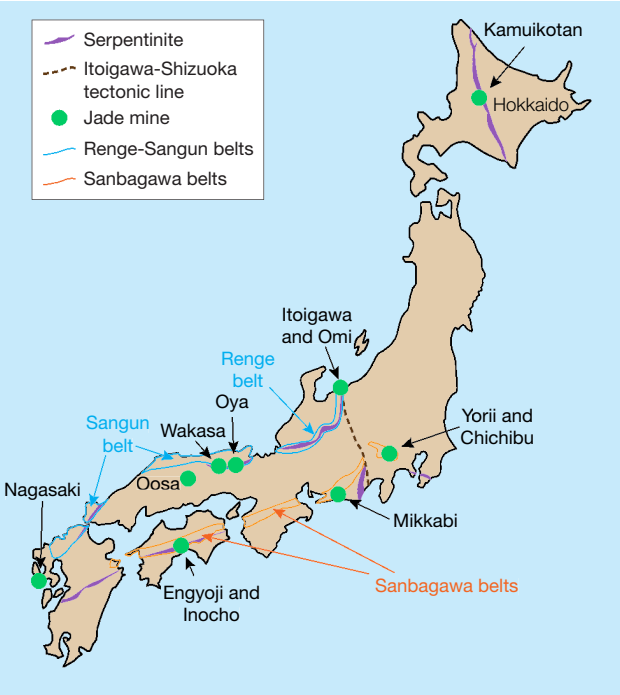

Figure 2. Japanese jadeite is found in eight locations, though the only significant source of gem-quality material is the Itoigawa-Omi region in Niigata Prefecture. Modified after Fossa Magna Museum.

the material's color varieties, internal texture, and chemical features using quantitative electron microprobe (EPMA) and laser ablation–inductively coupled plasma–mass spectroscopy (LA-ICP-MS) analysis.

HISTORICAL BACKGROUND

In addition to Japan, major jadeite localities include Myanmar, Russia, Central America, and the United States. Some of the world's earliest jadeite jade artifacts emerged from the Olmec, Maya, and Aztec civilizations of modern-day Mexico and Guatemala, which flourished from about 1200 BC until the Spanish conquest in the 16th century (Foshag and Leslie, 1955; Umehara, 1971; Taube, 2004). During the Jomon era, about 5,500 years ago, Japan's Itoigawa region became the birthplace of jadeite carving (figure 2), and it is no exaggeration to say that the Japanese gem culture was derived from this area. In the middle of the Jomon era, pendant-like jadeite pieces called *taishu* were produced and traded throughout many parts of Japan. Rough jadeite fashioning techniques, including spherical bead carving, were passed on in the late Jomon era. In the Yayoi era, curved *magatama* and tube-shaped *kudatama* beads became popular. According to legend dating from the early 8th century, the ancient state of Koshi (in modern-day Niigata Prefecture) was ruled by a beautiful empress who wore a mysterious curved green jadeite (figure 3). Koshi produced a variety of beautiful stones and cultivated a thriving trade with many other parts of Japan. Typically excavated from the tombs of powerful people, magatama jadeite appears to have been a sacred ornament as well as a symbol of wealth and prestige. Magatama carvings spread to the Korean Peninsula, where they have been excavated at many archaeological sites (Barnes, 1999).

Thousands of years of jadeite culture went into decline during the mid and late Kofun period (3rd to 7th century AD) before disappearing in the 6th century. Jadeite was rediscovered in Japan in 1938, more than a thousand years after vanishing, when researcher Eizo Ito uncovered it at the Kotaki River in the city of Itoigawa. The following year, Dr. Yoshi-

Figure 3. In this mosaic painting, made with pieces of Itoigawa jadeite, the magatama carving is worn by an empress of the ancient state of Koshi, in modern-day Niigata Prefecture. Courtesy of the Jade Ore Museum (Hisui Gensekikan).

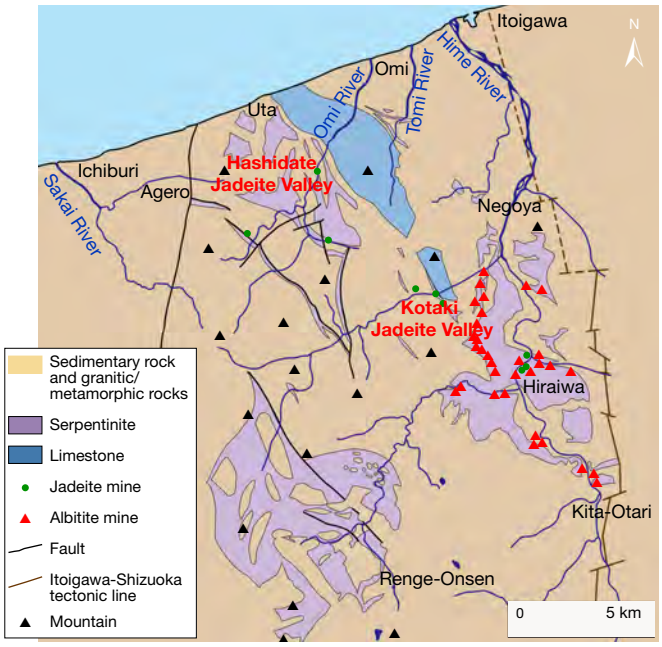

Figure 4. Jadeite from Itoigawa is found in serpentinite along a fault as blocks near the Kotaki River (upstream of the Hime River) and the Omi River. The Kotaki and Hashidate valleys are the main sources of gem-quality jadeite. White is the most common color, followed by green. Lavender, violet-blue, and blue jadeite are also found in Itoigawa-Omi. Source: Fossa Magna Museum.

nori Kawano and his colleagues at Tohoku University published a study of the samples (Kawano, 1939; Ohmori, 1939). Subsequent research led to additional discoveries in the Kotaki area, upstream of the Hime River, as well as in the Hashidate area of Itoigawa (figure 4). In 1954, some of these areas were designated as preservation sites, but jadeite is still found along these rivers or their estuaries.

Jadeite from Itoigawa, especially along the coast, is beautiful even in its rough state. Colors include white, green, violet, blue, and black. But because the sites are protected and mining is not allowed, there is little supply of this material in the market. In September 2016, Itoigawa jadeite was chosen as Japan's national stone by the Japan Association of Mineralogical Sciences.

JADEITE FROM JAPANESE LOCALITIES

Jadeite is found in high-pressure, low-temperature metamorphic belts (Essene, 1967; Chihara, 1971; Harlow and Sorensen, 2005). It is associated with kyanite, an indicator mineral of high-pressure, low-temperature metamorphism. The Japan Trench is a boundary between the Pacific plate and the Eurasia plate containing the Japanese islands, under which the cold Pacific plate subducts. This area is thought to have a high-pressure, low-temperature condition that produces jadeite. Japan has eight jadeite occurrences in all (again, see figure 2). Most of the jadeite from the Renge and Sangun belts on the western side (Itoigawa, Oosa, Oya, and Wakasa) is very pure, composed of more than 90% jadeite (including similar omphacite). Material from other parts of Japan very rarely contains more than 80% jadeite. Most contains large amounts of albite, kyanite, and analcime and no more than 50% jadeite (Yokoyama and Sameshima, 1982; Takayama, 1986; Miyazoe et al., 2009; Fukuyama et al., 2013).

Renge and Sangun Belts. The Itoigawa region is assigned to the Renge belt, a serpentinite mélange zone with various types of tectonic blocks, high-pressure and low-temperature metamorphic rocks, metamorphosed sedimentary rocks, amphibolites, and rodingites (Nakamizu et al., 1989). Gem-quality jadeite has been found only at the Kotaki and Hashidate districts in Itoigawa-Omi, occurring as boulders in the serpentinite located at the fault border between the Permian-Carboniferous limestone and Cretaceous sandstone and shale. Jadeite boulders range from one meter to several meters in size and are mostly distributed in an area several hundred meters long. Jadeite rocks in Kotaki show concentric zoning, toward the rim, of albitite (with or without quartz), white jadeite, green jadeite, soda-rich calciferous amphibole, and host serpentinite. Omi jadeite rock shows a "distinct stratiform structure," sometimes with alternating coarse and fine compact layers and often containing lavender jadeite (Chihara, 1991).

Sources other than Itoigawa in the Renge and Sangun belts (Oosa, Oya, and Wakasa) produce limited amounts of jadeite, most of it white with a few green areas. Green jadeite with high transparency has not been found in these areas. Considering that it contains similar minerals as well as zircons that are about 500 million years old (Tsutsumi et al., 2010), the material from Oosa, Oya, and Wakasa presumably formed through the same process as the Itoigawa jadeite. These fine-grained specimens cannot be differentiated microscopically from those of Itoigawa.

The Wakasa region in Tottori Prefecture of western Japan is a source of blue jadeite. Jadeite and jadeite pyroxene occur in serpentinites and metagabbros related to the Sangun regional metamorphic belt (Kanmera et al., 1980; Chihara, 1991). In this locality, jadeite rock

formed as a vein in part of a serpentinite body ranging from 5 to 30 cm in diameter. The rocks are mostly weathered but still hard and compact. Most of the jadeite has a violetish blue to blue, lavender, and milky white color and is associated with albite, quartz, and chlorite. Wakasa jadeite is also known to have a blue color, but production is very limited.

Hokkaido. The northern Japanese island of Hokkaido is shown in figure 2. The Kamuikotan belt, a high-pressure metamorphic belt, extends north to south in Hokkaido. In the serpentine area of this metamorphic belt in the Asahikawa district, jadeite-bearing rocks are very rare but may locally contain more than 80% jadeite. Most of the jadeite around 10 cm in size contains less than 50% jadeite content, however. Various mineral components deprive the jadeites of their transparency, making them difficult to distinguish from surrounding green rocks of lawsonite-albite facies retrograded in greenschist facies.

In Brief

- Japan's only source of gem-quality jadeite is the Itoigawa-Omi region in Niigata Prefecture. The area belongs to a serpentinite mélange zone with high-pressure and low-temperature metamorphic rocks, amphibolites, and jadeitites.
- Some 5,500 years ago, jadeite carvings were traded throughout Japan. Since the rediscovery of the jadeite source in 1938, limited quantities have been available.
- These Japanese jadeites display a variety of colors, including white, green, lavender, violetish blue, blue, and black. White jadeite shows a very pure jadeite component, while green jadeite has a low percentage of omphacite ranging from 2% to 18% and is colored by Fe and Cr. Blue samples are enriched with Ti.
- Trace element analysis by LA-ICP-MS confirmed that lavender, violetish blue, and blue jadeite showed higher large-ion lithophile elements and higher field strength elements than green, white, and black jadeite.

Sanbagawa Belt. Two deposits of jadeite-bearing rock have been reported in the Yorii and Chichibu districts in the Kanto Mountains of Saitama Prefecture. One of the locations forms a dome with serpentine, and the maximum jadeite content there is about 50%. Another occurrence, accompanied by actinolite rocks that supposedly replaced serpentinite, is similar to the surrounding metamorphic rocks where jadeite occurs in clusters, and samples with more than 80% jadeite content are rare. The jadeite from this area is not suitable for jewelry and, like material from Hokkaido, cannot be differentiated from the surrounding metamorphic rocks. Mikkabi in Shizuoka Prefecture also produces jadeite, found as a white vein 2 to 3 cm thick in metagabbro, but it too is unsuitable for fashioning.

Kochi and Nagasaki. Rocks containing jadeite have occasionally been found within serpentinite in the city of Kochi. These include gray quartz-bearing rocks and green rocks containing pumpellyite and kyanite. Neither contains more than 60% jadeite or possesses transparency, and thus cannot be visually differentiated from common hard metamorphic rocks. In Nagasaki, rocks containing jadeite associated with serpentine have been reported. Parts of the rock contain more than 80% jadeite, but the content is often as low as 50%. Only limited amounts of the jadeite-bearing rocks have been produced.

SAMPLE DESCRIPTIONS AND ANALYTICAL METHODS

To examine the color varieties of Japanese jadeite, we collected representative samples from the field in Itoigawa and Wakasa and from the Jade Ore Museum (Hisui Genseki Kan) in Tokyo and the Fossa Magna Museum in Itoigawa (see the top table at https://www.gia.edu/gems-gemology/spring-2017-japanese-jadeite-tables). The 39 rough and cut Japanese samples consisted of white, green, dark green, lavender, violetish blue, blue, and black jadeite. They were from three different sources: the Kotaki River area (36º55'33N, 137º49'18E; 32 samples) and Hashidate (36º58'35N, 137º45'51E; five samples), both in Itoigawa, and the Wakasa region (35º32'17N, 134º44'52E; two samples).

To compare their optical features, petrographic structures, and geochemistry with samples from other parts of the world, we also tested Russian white and green jadeite from the Polar Urals (four samples); dark yellowish green and lavender jadeite from the Motagua region of Guatemala (six samples); and Burmese white, green, and lavender jadeite from Kachin State (38 samples). The samples were provided by the Jade Ore Museum (Hisui Gensekikan) and Miyuki Co., Ltd. Examples are shown in figure 5.

All 87 samples were observed by visual and microscopic means, and their refractive indices were examined by either normal reading from flat wafers or by the spot method. Specific gravity was determined

Figure 5. Representative samples from four locations. A: Magatama carvings (25.51–63.88 ct) from Itoigawa-Omi. B: Variously colored rough jadeite boulder, cobble, and pebbles from Itoigawa-Omi (15.3–622.2 g) and a polished violetish blue jadeite from the Wakasa region (458.2 g). C: Green and lavender cabochons (4.75–15.45 ct) and polished slices from Kachin, Myanmar (17.84–136.4 g). D: Rough grayish green and lavender jadeite blocks from the Motagua region of Guatemala (223–1250 g). E: A green jadeite block (304 g) and two polished translucent to opaque jadeites (139.08 and 5.93 ct) from the Polar Urals of Russia. The magatama from Itoigawa-Omi and the Russian and Guatemalan samples are courtesy of the Jade Ore Museum (Hisui Gensekikan). The Burmese jadeites are courtesy of Miyuki Co., Ltd. Photos by Masumi Saito and Ahmadjan Abduriyim.

hydrostatically for all the samples, and their absorption spectra were observed by handheld prism spectroscope. Four inclusion-bearing samples from Itoigawa and Wakasa, three from Kachin, two from Motagua, and two from the Polar Urals were cut and polished into thin sections for petrographic structure

analysis. The micro-texture of these petrographic thin sections was observed using a Nikon Optiphot polarized light microscope.

To identify the inclusions and reveal the distribution of jadeite and other minerals in jadeite rock, we used a two-dimensional micro-Raman mapping spectroscope (Horiba Jobin Yvon XploRA LabRAM HR Evolution) equipped with a 532 nm Nd:YAG laser and an optical microscope (Olympus BX41) under real usage conditions. The laser beam was narrowed and focused through a 300 µm aperture and a 100× objective lens, yielding a spatial resolution of about 1 µm. Raman spectra were acquired with a single polychrome spectrometer equipped with a Si-based charge-coupled device (CCD) detector (1024 × 256 pixels). A composite spectrum in the range of 200–1800 cm^{-1} was obtained with LabSpec software, using a 600 gr/mm grating with a spectral resolution of about ±2.5 to 3.5 cm^{-1}. Before performing the measurements, we calibrated the spectrometer by the Si 520 cm^{-1} peak. Raman spectral mapping was conducted in point-by-point macro mode using XY stepping motors. It took 15 minutes to obtain a 44 × 30 mm spectral macro mapping image with a step size of 500 µm in the 200–1800 cm^{-1} range.

UV-Vis-NIR spectroscopy was performed on parallel polished wafers of green, lavender, and blue samples from Kotaki, Itoigawa; a violetish blue sample from the Wakasa region; green and lavender samples from Kachin and Motagua; and a green sample from the Polar Urals. The analyses were performed using a Hitachi U-2900 spectrophotometer at 1 nm resolution. The parallel polished plates were oriented with the main polished face perpendicular to the instrument beam, and the polarizer was not rotated. The thin sections ranged from 3.63 to 10.08 ct and from 0.86 to 3.70 mm thick.

To investigate the various colors of the jadeites, very precise quantitative chemical composition measurements were obtained by electron microprobe with wavelength-dispersive spectrometry (WDS) mode (JEOL LXA-8900) at the University of Tokyo and Waseda University. Eleven thin sections and polished thin plates from Itoigawa and Wakasa, two specimens from Motagua, and one specimen from the Polar Urals were analyzed with 15 kV accelerating voltage, using a beam current of 12 nA and beam diameter of 10 µm. Data were processed with ZAF correction software. The standards were natural albite for Al(Kα) and Na(Kα), wollastonite for Ca(Kα) and Si(Kα), orthoclase for K(Kα), chromite for Cr(Kα), Mn-olivine for Mn(Kα), and TiO_2, Fe_2O_3, MgO, and NiO for Ti(Kα), Fe(Kα), Mg(Kα), and Ni(Kα), respectively.

Trace element and rare earth element (REE) analyses were performed with LA-ICP-MS using a Thermo Scientific iCAP Q quadrupole ICP-MS with an ESI UP213 Nd-YAG laser. The laser repetition rate was 7 Hz, with an energy density of 10 J/cm^2 and a spot size of 40 µm, using a carrier gas mixture of helium and argon. It was possible to detect the signal of all isotope ratios and achieve an analytical precision of less than 10% relative standard deviation (RSD). Three to ten spots were ablated for each sample, and averaged data was calibrated. NIST SRM 610 and 612 were used as external standards. Before analysis, the samples were cleaned with acetone and aqua regia in an ultrasonic bath to eliminate surface contamination.

RESULTS AND DISCUSSION

Gemological Observations. Jadeite pebbles from Itoigawa-Omi tend to have rounded corners, resulting from erosion by fluvial processes, and a glittering whitish surface. Because of surface weathering, the rough rock does not have a brown skin. These stones are mainly white, with unevenly distributed pale green to green areas, and they feel rigid, compact, and heavy. Most of the white rocks mixed with some green were in boulder, pebble, and nodule form, transparent to semi-translucent to opaque, and finely textured, with some coarse texture in eye-visible single crystals. The largest rough specimen, found in the Hashidate district, weighed 102 tons. The author has also observed a 4.6 ton jadeite rock from the Kotaki district that is housed in the Fossa Magna Museum (figure 6, left). In this large jadeite boulder, most of the white and green parts were jadeite jade, while the fibrous black portion was composed of amphibole. Some small green areas were translucent and gemmy. Some minor faults were filled with white minerals such as prehnite, pectolite, and zeolite-group minerals that formed within fluids from the deeper part of the earth.

In lavender jade, the violet color may be dispersed irregularly over the white matrix. This color is semi-translucent to opaque, with a fine to medium texture (figure 6, center). The blue jadeite samples, found in a variety of beautiful colors, were rounded and semi-translucent to opaque, with fine to coarse texture (figure 6, right). Aggregates of minute crystals were observed through a loupe but lacked crystal form. Specimens from Itoigawa and Tottori had a spot RI of 1.65 to 1.66 and SG values ranging from 3.10 to 3.35. Green jadeite samples were inert under long-wave

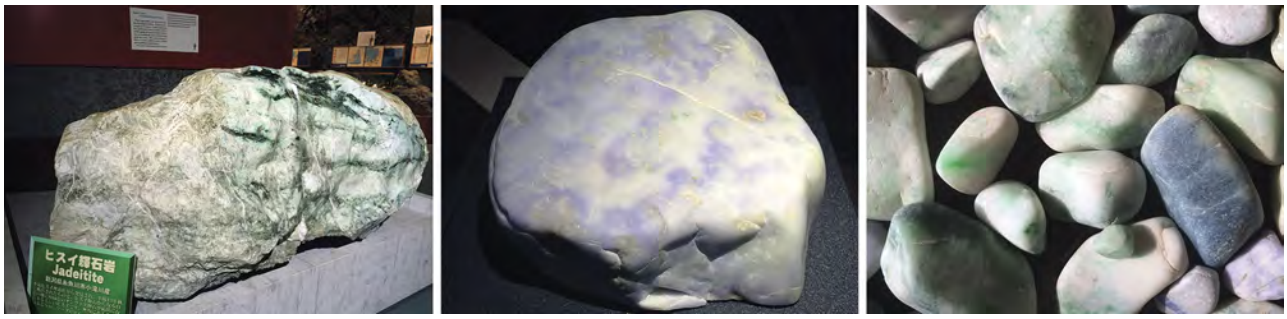

Figure 6. Left: A 4.6 ton jadeite rough boulder is displayed at the Fossa Magna Museum in Itoigawa. This eroded and rounded boulder from the Kotaki area is mostly white, with some green areas of jadeite; the fibrous structure in the black area is amphibole. Thin fault-like veins are filled with white minerals. Center: A 30 kg rounded boulder of predominantly lavender jadeite was found along the Hime River in Itoigawa. The lavender color is dispersed irregularly over the white matrix. Right: These rounded jadeite pebbles, found along the coast in Itoigawa-Omi, are approximately 2 to 15 cm long. Photos by Ahmadjan Abduriyim, courtesy of the Fossa Magna Museum and the Jade Ore Museum (Hisui Gensekikan).

(365 nm) and short-wave (254 nm) UV radiation. The lavender jadeite exhibited a stronger reddish fluorescence than Burmese lavender jadeite, which showed a weak reddish fluorescence to long-wave UV. The Japanese blue jadeite was inert to both long- and short-wave UV. The absorption spectra of all Japanese jadeite samples, measured by a handheld spectroscope, revealed weaker lines at 690, 650, and 630 nm. In addition, green jadeite from Itoigawa showed a very sharp line at 437 nm. The lavender jadeite showed weak bands at around 530 and 600 nm and a narrow band at 437 nm. The blue jadeite showed a very broad band from the yellow to red portion of the spectrum, as well as a weak narrow band at 437 nm.

The representative Guatemalan jadeite samples selected for this study were grayish and dark green, white, and violetish blue. The green rough was semi-translucent and opaque, with a fine to medium-grained texture but also somewhat coarsely grained texture in visible crystals. The "Olmec blue" rough from Guatemala was variegated violet to blue mixed with abundant white color. It was translucent to opaque, with a fine texture. Its color distribution closely resembled that of Japanese lavender and blue jade.

Jadeite from the Polar Urals occurs in different shades of green. The material usually has a more even color distribution than Japanese green jadeite, and it is highly valued. The samples from this source were semitransparent to translucent, with a fine to medium texture. Black spots of magnetite could be observed.

Petrographic Observation. In plane-polarized light, a white and green jadeite slice from Itoigawa (K-IT-JP-14; see figure 7-A1) revealed colorless, semitransparent jadeite crystals distributed in the white area, mostly as fine cryptocrystalline grains around 0.05–0.3 mm in size. Under cross-polarized light, the fine jadeite grains showed both high- and low-order interference colors, caused by the different orientation of each grain. Under plane-polarized light, we occasionally observed in matrix large pale green grains over 2 mm (figure 7-A2) that were well-formed jadeite single crystals. Their well-developed cleavages intersected at 87° angles, which is characteristic of pyroxene. This thin section of green jadeite showed a prismatic crystalloblastic texture, indicating metamorphism under nondirectional pressure. Micro-Raman spectrometry in microfolds and veinlets identified minor amounts of pectolite and prehnite as component minerals.

The thin section of lavender jadeite from Itoigawa-Omi was almost colorless under plane-polarized light (see figure 7-B1). The sample was semi-transparent to translucent and mainly composed of fine to micro-grained crystals around 0.1–0.3 mm in size, showing a prismatic crystalloblastic texture. Ultramylonitic zones with radiating aggregates of fine jadeite grains randomly cutting through the matrix were observed in this sample (figure 7-B2). This texture indicates that the sample underwent lithostatic and possibly subsequent directional pressure during the metamorphic process. Prehnite and analcime, the main constituents of the veinlets that cut through the jadeite rock (figure 7-B3), were formed by hydrothermal fluids (Shoji and Kobayashi, 1988). A long prismatic vesuvianite crystal with high relief was also found as a component mineral.

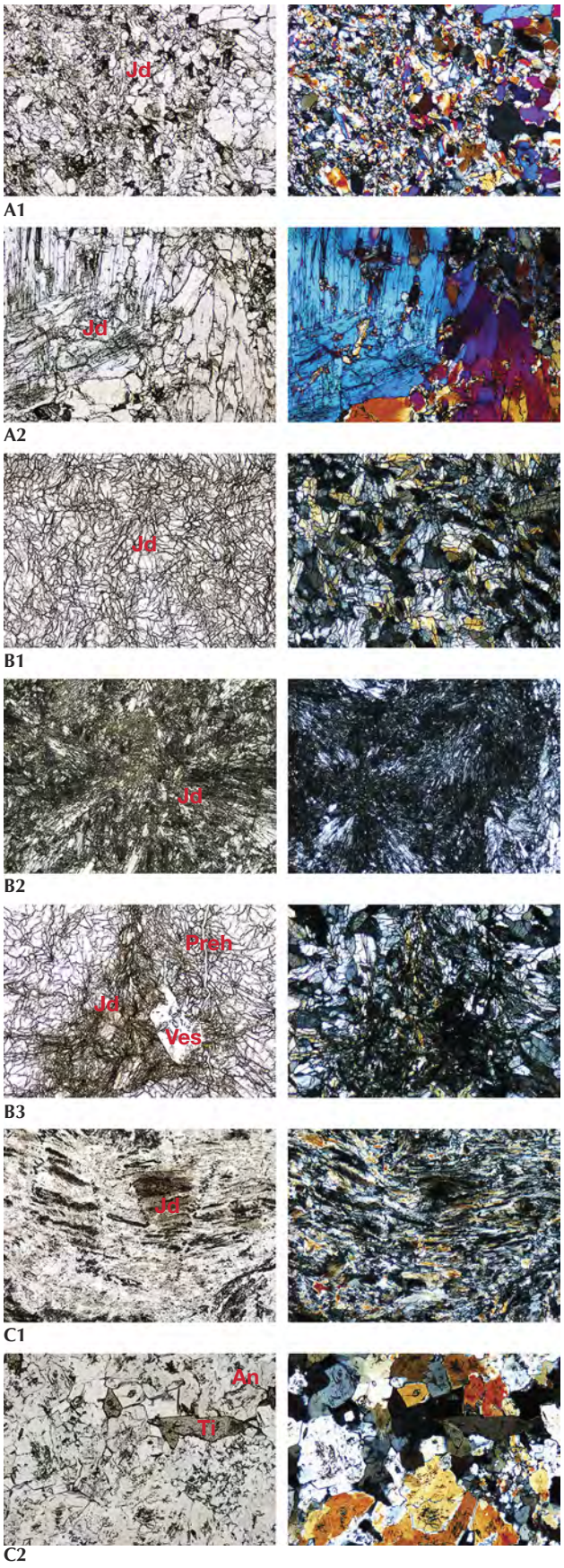

Figure 7. Petrographic microscope images of jadeite samples from Itoigawa. The left images are under plane-polarized light, the right images under cross-polarized light. Jd, Preh, Ves, An, *and* Ti *indicate jadeite, prehnite, vesuvianite, analcime, and titanite, respectively. A1: Green jadeite K-IT-JP-14 shows a prismatic-granular crystalloblastic texture, a distribution of fine colorless cryptocrystalline grains of jadeite, and a predominance of grains around 0.05–0.3 mm in size. A2: Coarse pale green grains larger than 2 mm can also be observed in the same matrix, which is a well-formed large jadeite single crystal. The prominent (110) cleavage planes intersecting at 87° are characteristic of pyroxene. B1: Lavender jadeite K-IT-JP-25 shows near-colorless fine and micro-grained jadeite crystals with a prismatic crystalloblastic texture. B2: Ultramylonitic zones with radiating aggregates of fine jadeite grains cut randomly through the center of the matrix, indicating a lithostatic pressure during the metamorphic process. B3: Dark gray prehnite and analcime, the main constituents of the veinlets that cut through this lavender jadeite, were formed by hydrothermal fluids. A high-relief prismatic vesuvianite crystal was also found as a component mineral. C1: K-IT-JP-16 is a predominantly blue specimen, translucent with fine cryptocrystalline grains. C2: Crushed preexisting minerals produce a flow structure with granoblastic and mylonitic texture. The component minerals analcime and a very minor amount of euhedral titanite grains are observed in the matrix. Photomicrographs by Ahmadjan Abduriyim.*

In the blue jadeite sample (K-IT-JP-16), the blue area was larger than the white area, and the colors gradually blended. It was translucent and granular, and the fine cryptocrystalline grains from 0.1 to 0.5 mm (figure 7-C1) showed granoblastic and mylonitic texture. In this specimen, preexisting minerals were crushed and slipped to produce a flow structure (figure 7-C2). Component minerals included analcime and titanite, as well as very minor amounts of euhedral titanite grains in the matrix that do not contribute to the blue color in this type of jadeite.

Morishita et al. (2007) proposed that jadeite from Itoigawa-Omi formed either by direct precipitation of minerals from aqueous fluids or by complete metasomatic modification of the precursor rocks by fluids. The Burmese green and lavender jadeite samples showed amphibole, albite, kosmochlor, and nepheline, while vesuvianite was rare. The Guatemalan green and lavender jadeite in this study showed grossular garnet, albite, and rutile, while the Russian green jadeite contained magnetite and analcime.

We used two-dimensional point-by-point Raman macro mapping to reveal the distribution of jadeite and other component minerals in the jadeite rocks.

Figure 8 shows a white and green/dark green sample from Itoigawa; the red, green, and blue colors correspond to the integrated intensity of jadeite, amphibole (richterite), and prehnite, respectively. This image reveals that the jadeite and amphibole grains are mixed within the matrix, while prehnite occurs in the vein. The rapid point-by-point confocal mapping technique can be performed on a whole specimen or a region of interest to examine finer details, making it possible to classify the distribution of jadeite vs. omphacite and/or amphibole.

UV-Vis Spectroscopy. *Japan*. UV-Vis absorption spectroscopy was performed on the green, violet, violetish blue, and blue jadeite wafers from the Itoigawa-Omi and Wakasa regions. Chemical analysis was carried out on similarly colored areas of the sample to confirm each chromophore's concentration.

Green portions of Itoigawa jadeite are generally colored by chromium and iron, showing a 691 nm absorption line (the Cr^{3+} "chromium line") and another absorption line that originates at around 437 nm (the Fe^{3+} "jadeite line"); see figure 9. The chromophore concentrations in the tested area, a 5 mm circle, were analyzed by LA-ICP-MS, and a concentration was averaged from three to four laser ablation spots. The green area contained relatively high Cr and Fe (280 and 810 ppma), and the isovalent chromophores Cr^{3+} and Fe^{3+} clearly contributed to the green color (Rossman, 1974; Harlow and Olds, 1987). The less significant chromophores Ti, Mn, V, and Co had lower concentrations (57, 19, 2.3, and 0.4 ppma, respectively; see the bottom table at https://www.gia.edu/gems-gemology/spring-2017-japanese-jadeite-tables).

The UV-Vis spectra of lavender jadeite from Itoigawa-Omi show features that correspond with Mn, Ti, and Fe (figure 10). A broad Mn^{3+}-related absorption band centered at 530 nm is often observed in Burmese lavender jadeite (Lu, 2012), as well as a characteristic broad band of paired Ti^{4+}-Fe^{2+} charge-transfer ions centered at 610 nm and a narrow Fe^{3+}-related 437 nm absorption band. The color-causing transition elements were analyzed in this lavender jadeite. The results showed that Ti (534 ppma average) and Fe (550 ppma average) were clearly responsible for its blue hue. Mn concentrations averaged 18 ppma and produced a weak pink or purple hue. The Japanese lavender jadeite showed a violet color, owing to the combination of minor pink and significant blue hues caused by Mn^{3+} and Ti^{4+}-Fe^{2+} absorption. Shinno and Oba (1993) discussed the substitution of Ti^{3+} at 545 nm in lavender jadeite from Itoigawa-Omi. However, the Ti^{3+} ion is very unstable in nature and is found only in meteorites and lunar samples formed in more reducing conditions (Burns, 1981). In terms of ionic radius, isovalent Ti^{3+} is noticeably larger than Al^{3+} and does not replace it in the six-fold coordinated octahedral site (figure 11). The chromophore concentrations of Ti and Fe in the violet parts reached 550 and 534 ppma, and this combination caused a noticeable blue color.

The UV-Vis spectra of blue jadeite from Itoigawa show a very broad band from 500 to 750 nm, a weak

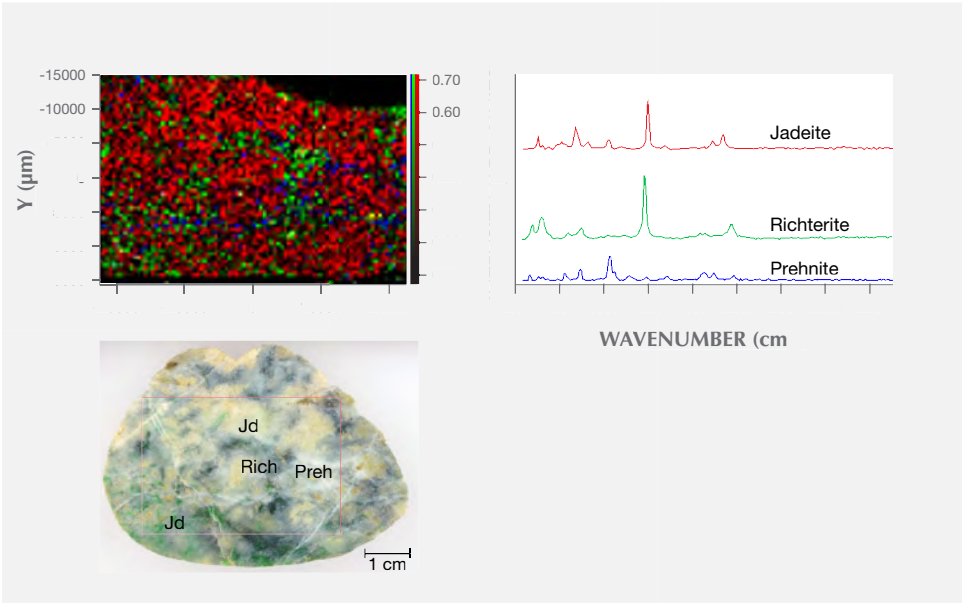

Figure 8. A two-dimensional Raman spectroscopy mapping image of a jadeite boulder from Itoigawa. The red area corresponds to the jadeite distribution, the green area to dark green richterite (amphibole group), and the blue area to the mineral prehnite, which is located at the veinlet and crosses through the stone. The mapping area is 44 × 30 mm.

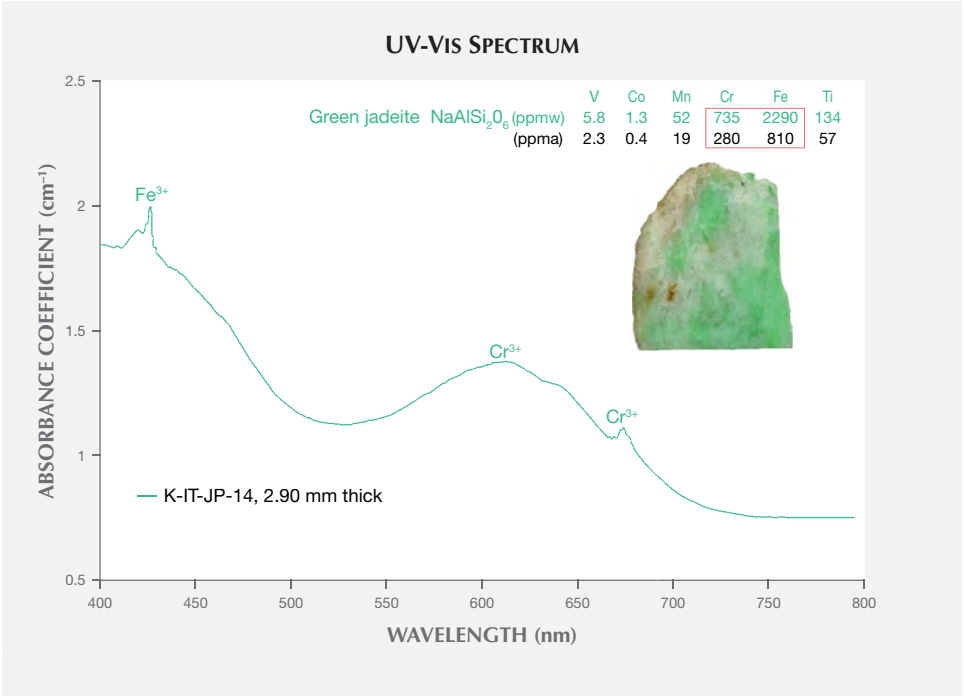

Figure 9. The UV-Vis spectrum of a green sample from Itoigawa (K-IT-JP-14) shows the features corresponding to Cr- and Fe-bearing green jadeite: the characteristic narrow 691 nm absorption, two Cr^{3+}-related weak shoulders at 650 and 630 nm, and a sharp, narrow absorption of Fe^{3+} at 437 nm. The saturated green area of the spectrum corresponds to the concentration of the chromophores Cr and Fe (280 and 810 ppma, on average).

Fe^{3+} absorption at 437 nm, and a cutoff above 350 nm (figure 12). This absorption pattern is similar to the spectra of blue sapphire and can be attributed to a charge transfer between Ti^{4+}-Fe^{2+} pairs (Ferguson and Fielding, 1971). Significant amounts of Ti (1943 ppma) and Fe (4212 ppma) produced a noticeable blue color. By comparison, Mn was too low (64 ppma) to produce a pinkish component.

The violetish blue jadeite from Wakasa in Tottori Prefecture showed a similar spectral characteristic, with lower Ti, Fe, and Mn concentrations than blue jadeite but higher concentrations than violet

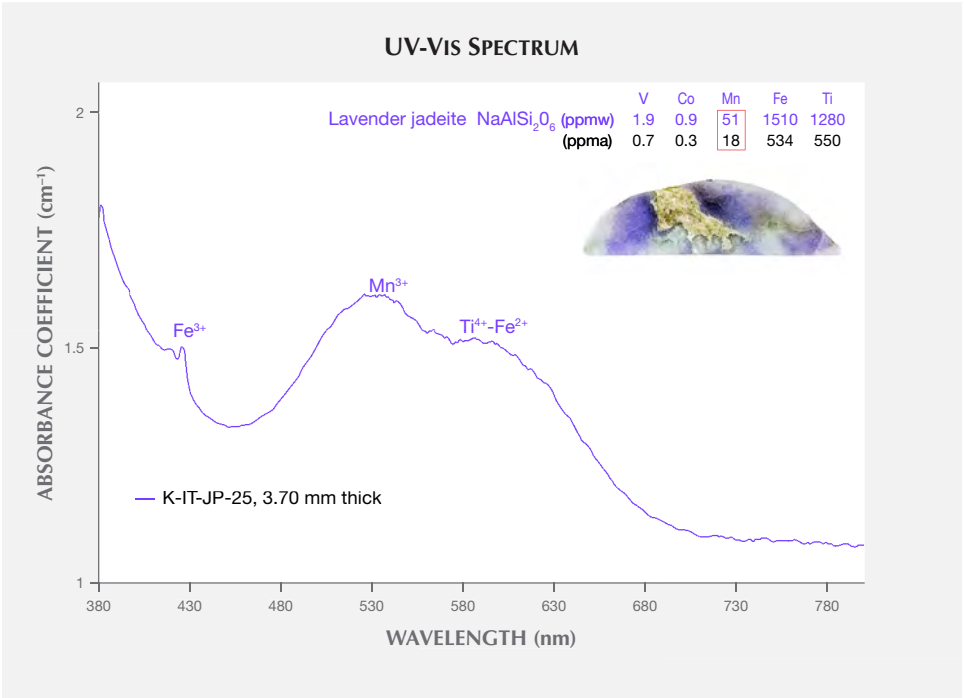

Figure 10. The UV-Vis spectrum of a lavender sample from Itoigawa-Omi (K-IT-JP-25). Two broad bands centered at 530 and 610 nm correspond to Mn and Ti-Fe charge transfer, and there is also a weak narrow band at 437 nm. The violet color reflects the chromophore combination of low Mn (18 ppma) and much higher Ti (534 ppma) and Fe (550 ppma).

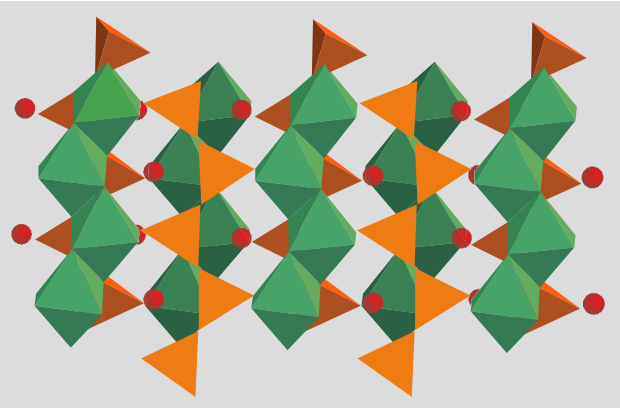

Figure 11. Illustration of the atomic arrangement of a single-chain pyroxene crystal structure, from the a-axis to b-axis direction. In the SiO_4 tetrahedrons (indicated in yellow and brown), four oxygen atoms surrounding a silicon atom are connected to form a strand, and other six-coordinate octahedron atoms (in green) are arranged so that they link the strands. Larger atoms (orange spheres) fill the spaces. Modified after Miyawaki (2004).

jadeite from Itoigawa (see the bottom table at https://www.gia.edu/gems-gemology/spring-2017-japanese-jadeite-tables).

Myanmar. The UV-Vis spectrum of the Burmese green jadeite (K-MYA-16) showed the characteristic narrow Cr^{3+}-related absorption band at 691 nm and the sharp, narrow Fe^{3+}-related absorption band at 437 nm that is very common in natural green jadeite. The Cr and Fe absorption feature generally overlapped with the spectrum of Japanese green jadeite, but the absorption intensity was much higher in Burmese jadeite due to its color saturation and transparency (figure 13A). The Burmese lavender jadeite (K-MYA-20) with a predominantly purple color component had a broad absorption centered at 570 nm, related to Mn concentration (figure 13B). The Fe and Ti concentration was much lower than in Japanese lavender jadeite and might not cause any noticeable blue component.

Guatemala. Only the characteristic Fe^{3+}-related narrow absorption band at 437 nm was found in the Guatemalan grayish green jadeite spectrum, which lacked the Cr^{3+} absorption (figure 13C). A very closely matched absorption spectrum was observed in Guatemalan lavender jadeite, which showed multiple broad bands centered at 530 and 610 nm and a weak narrow band at 437 nm (figure 13D). This absorption feature, related to Mn^{3+}, Ti^{4+}-Fe^{2+} pairs, and Fe^{3+}, generally overlapped with the bands observed in Itoigawa lavender jadeite. The concentrations of V, Cr, and Co were too low to create any noticeable color.

Russia. A highly saturated vivid green jadeite from the Polar Urals showed an Fe^{3+} band and strong multiple chromium lines in the 580–700 nm range, a

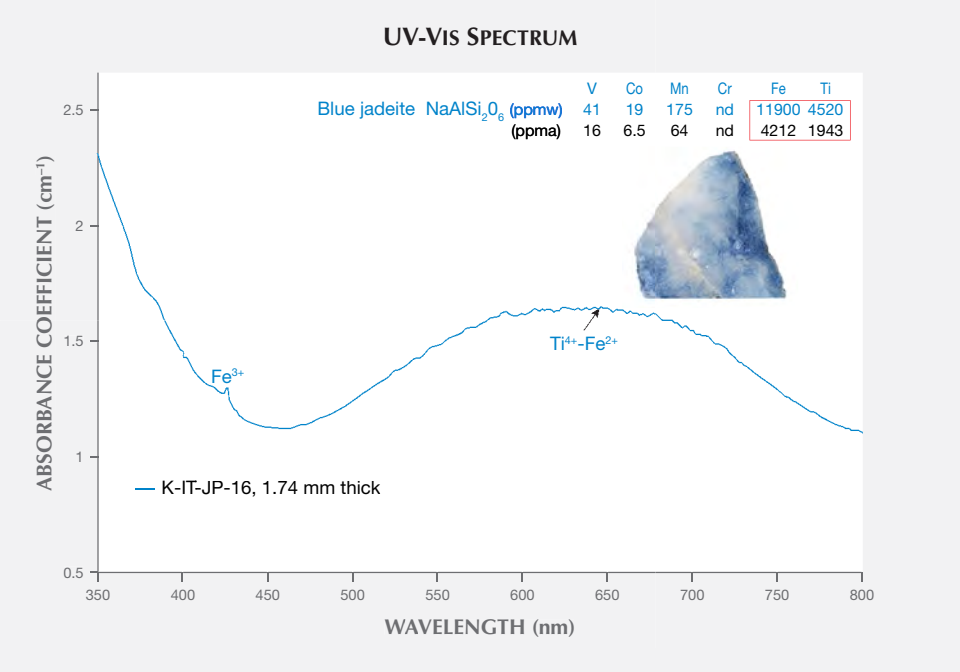

Figure 12. The UV-Vis spectrum of a blue sample from Itoigawa (K-IT-JP-16). The absorption shows a very wide broad band from 500 to 750 nm that overlaps the Mn-related broad bands at 530 and 570 nm observed in Burmese lavender jadeite. The chromophores Ti and Fe show a significant concentration at 1943 and 4212 ppma, respectively, and this jadeite's blue color could be mainly due to the Ti^{4+}-Fe^{2+} charge transfer.

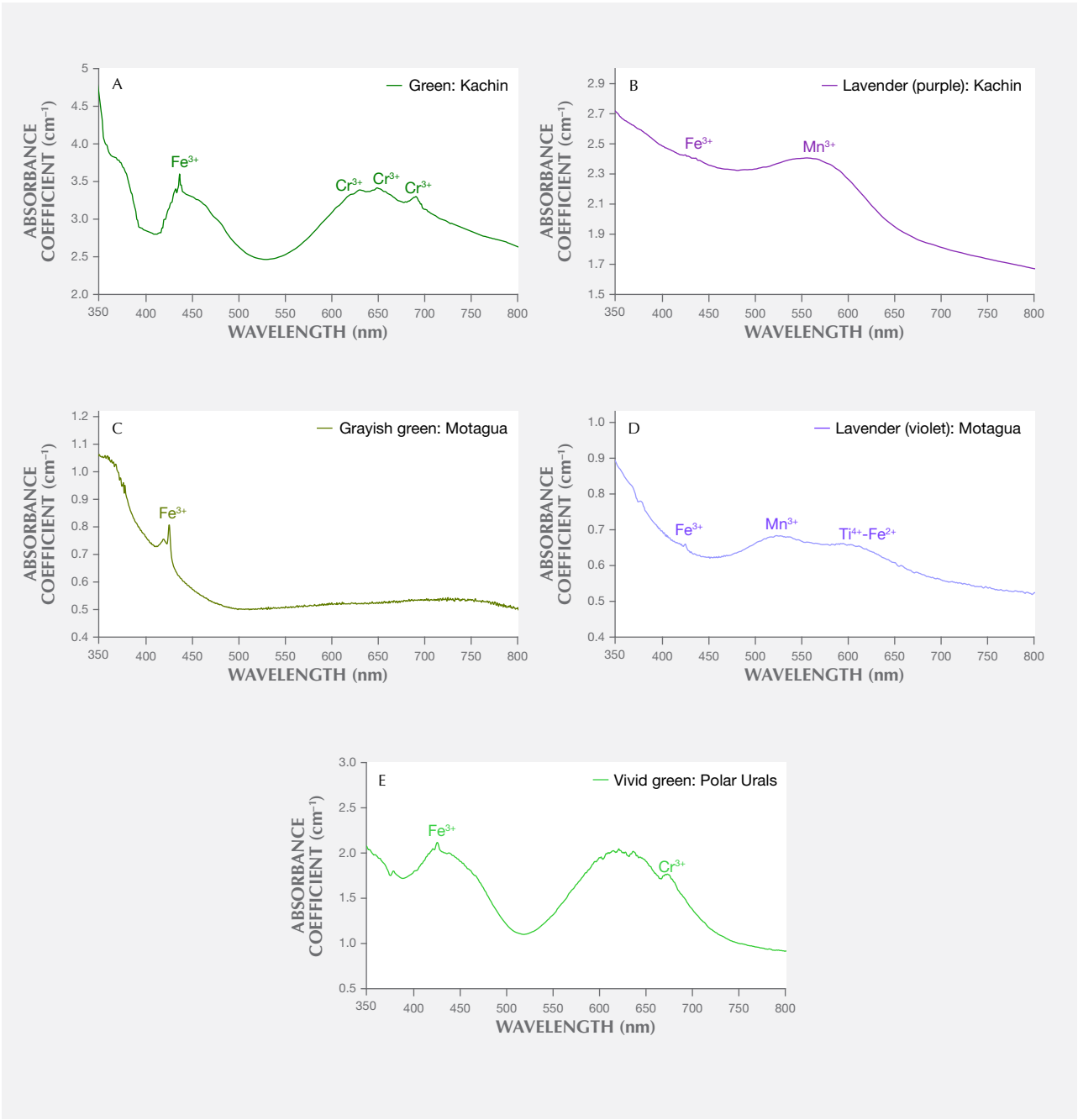

Figure 13. A: The UV-Vis spectrum of a green Burmese jadeite (K-MYA-16) shows the characteristic chromium lines at 630, 650, and 691 nm and the sharp, narrow Fe^{3+} absorption band at 437 nm that is commonly seen in natural green jadeite. The Cr^{3+}- and Fe^{3+}-related feature generally overlaps with the spectrum of Japanese green jadeite, but the absorption intensity is much higher due to its color saturation and transparency. B: Burmese lavender jadeite (K-MYA-20) showed a dominant broad absorption band centered at 570 nm, related to Mn^{3+} concentration. C: The narrow Fe^{3+} absorption band at 437 nm, often present in Guatemalan green jadeite (M-GUA-02). The absorption of Cr^{3+} is not detectable in this 2.32-mm-thick sample. D: The spectrum of Guatemalan lavender jadeite (M-GUA-03) shows multiple broad bands centered at 530 and 610 nm and a weak narrow band at 437 nm. The absorption feature related to Mn^{3+}, Ti^{4+}-Fe^{2+}, and Fe^{3+} generally overlaps with the bands observed in Itoigawa lavender jadeite. E: A vivid green Polar Ural jadeite shows an Fe^{3+} band and strong multiple chromium lines in the 580–700 nm range, a combination that typically produces a highly saturated green color. The concentration of Cr (maximum of 3042 ppma) is much higher than in Japanese green jadeite.

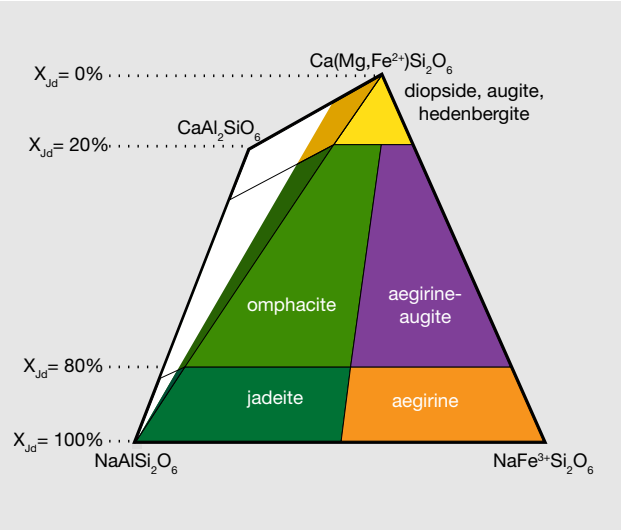

Figure 14. This classification of pyroxene based on chemical composition shows the relationship between jadeite and other pyroxenes in the main isomorphous substitution. Source: National Museum of Nature and Science, Tokyo.

combination that typically produces a highly saturated green color (figure 13E). The Cr concentration (up to 3042 ppma) was much higher than in Japanese green jadeite.

Chemical Analysis. Quantitative chemical data collected by EPMA for the samples from Japan, Guatemala, and Russia are summarized in table 1. The results are described below for each representative color: white, green, lavender, and blue (including violetish blue). X_{Jd}, $X_{[Ae+Ko]}$, and $X_{Quad\ [Dio+Aug+Hed]}$ were calculated as mol.% of Al/(Na + Ca), Fe^{3+}/(Na + Ca), and Ca/(Na + Ca), respectively (figure 14). The highest and lowest concentrations of jadeite (X_{Jd}) for 11 tested samples are listed in table 1. The 87 specimens from the four countries in this study (Japan, Myanmar, Guatemala, and Russia) were analyzed by LA-ICP-MS, with averaged data calculated based on three to ten laser ablation spots for each specimen; minimum and maximum values of each element concentration are listed in the bottom table at https://www.gia.edu/gems-gemology/spring-2017-japanese-jadeite-tables, with averaged data in parentheses.

White Jadeite. White jadeite from Itoigawa belongs to the clinopyroxene group and is close to the ideal jadeite composition (again, see table 1). All analyses (more than five spots) were close to the end member composition, up to X_{Jd} = 98 mol.%. The CaO, MgO, and FeO_{tot} contents were lower than those tested from any other jade color (0.26, 0.12, and 0.44 wt.%, respectively). Values for Cr_2O_3, MnO, K_2O, and NiO were below the detection limit of the analysis. TiO_2 (0.03 wt.%) was lower than values analyzed from violet and blue jadeite elsewhere. The white jadeite was very pure.

LA-ICP-MS analyses of the white jadeite consistently identified 19 minor and trace elements (Li, Mg, K, Ca, Sc, Ti, V, Cr, Mn, Fe, Co, Cu, Sc, Ni, Zn, Ga, Se, Sr, and Zr). Other trace elements (B, Rb, Y, Nb, Sm, Eu, Gd, Tb, Dy, Ho, Er, Tm, Yb, Lu, Hf, Ta, W, Th, and U) were above the detection limits. Although Itoigawa "white" jadeite generally had lower Mg and Ca contents (3841 and 8495 ppmw, respectively) than green, blue, and black jadeite, almost all of the detectable minor and trace element contents were higher than in white jadeite from Kachin State in Myanmar (see the bottom table at https://www.gia.edu/gems-gemology/spring-2017-japanese-jadeite-tables).

Green Jadeite. Microprobe analyses of four green jadeites revealed significant Fe content, from a minimum value of 0.22 wt.% to a maximum of 0.864 wt.%, and a slightly low Cr value of 0.01–0.57 wt.%. Values for MgO (0.16–2.83 wt.%) and CaO (0.24–4.18 wt.%) were relatively high, but the compositions fit within the jadeite range of X_{Jd} = 98.7 to 82.4 (figure 15). Samples from Itoigawa-Omi showed slight differences in major element composition between crystal aggregates and discrete single-mineral grains. This study indicates that the green jadeite is also nearly pure jadeite, though some discrete single-mineral grains showed a composition closer to omphacite within the jadeite-dominant matrix.

The 13 green specimens from Itoigawa revealed the remarkable transport of large-ion lithophile elements in subduction zones, such as Li, B, K, Sr, and Ba, as well as elements that are considered more refractory, such as rare earth elements (La, Ce, Pr, Nd, Sm, Eu, Gd, Tb, Dy, Ho, Er, Tm, Yb, and Lu) and Hf, Ta, W, Tl, Pb, Th, and U. The Mg and Ca contents were also relatively high, ranging from 2383 to 77,100 ppmw for Mg (averaged to 19,957 ppmw) and 4400 to 82,700 ppmw for Ca (averaged to 39,206 ppmw). Mg and Ca contents were much higher in the dark green areas, which indicates that the dark green omphacite component is more abundant in trace elements (except Li and Ga) than jadeite. To establish a useful chemical fingerprint diagram for separating omphacite jade from jadeite jade, we plotted two different combinations of major and minor elements. As seen in figure 16, plot-

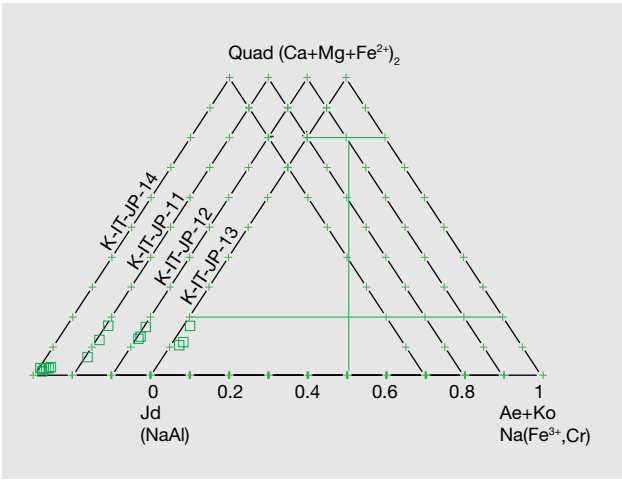

Figure 15. This ternary diagram for jadeite (Jd)-aegirine + kosmochlor (Ae + Ko)-Ca-Fe-Mg pyroxene (diopside + augite + hedenbergite) indicates the chemical concentration data of four green jadeites from Itoigawa-Omi by EPMA, based on Morimoto et al. (1988). Their compositions fit the jadeite range of X_{Jd} = 98.7 to 82.4. Three to 12 spots were tested on the green area of each specimen.

ting Al/Fe vs. Ca/Na clearly separates the jadeite according to chemical concentration.

By comparison, the green samples from Itoigawa-Omi showed higher Li, B, Mg, K, Ca, Ni, and Sr than green jadeite from Myanmar, while the transition metal elements Ti, V, Cr, Mn, Fe, and Co showed similar ranges. Ti and Fe were dominant in Russian and Guatemalan green jadeite. The Russian green jadeite showed the highest Cr content (up to 7940 ppmw, averaged to 2872 ppmw) of any samples.

Lavender Jadeite. EPMA performed on a violet sample from Itoigawa (K-IT-25) yielded significant TiO_2 (up to 0.362 wt.%) and FeO_{tot} (up to 0.694 wt.%), whereas MnO was relatively low (up to 0.019 wt.%). The color of the Japanese lavender jadeite likewise should correlate to the chromophores Ti^{4+}, Fe^{2+}, and Mn^{3+}. The contents of MgO (up to 0.864 wt.%) and CaO (up to 1.879 wt.%) were relatively low. The jadeite composition ranged from X_{Jd} = 98.7 to 93.3, close to pure jadeite.

LA-ICP-MS detected noticeably high amounts of Ti and Fe in all of the violet jadeite. Other metal elements such as Li, B, K, Sr, and Ba, as well as REEs, were higher than in white or green jadeite from the same geological source in Itoigawa-Omi. Lavender jadeite from Guatemala showed a similar violetish hue, and trace element concentrations revealed similarly high levels of Ti and REEs. But the transition metal ions V, Cr, and Co were below detection limits, consistent with its original light violet color (Sorensen et al., 2003). By comparison, 16 Burmese lavender samples showed appreciable Mn, explaining their dominant pinkish/purplish component. Oberhänsli et al. (2007) did not observe a Ti phase in the

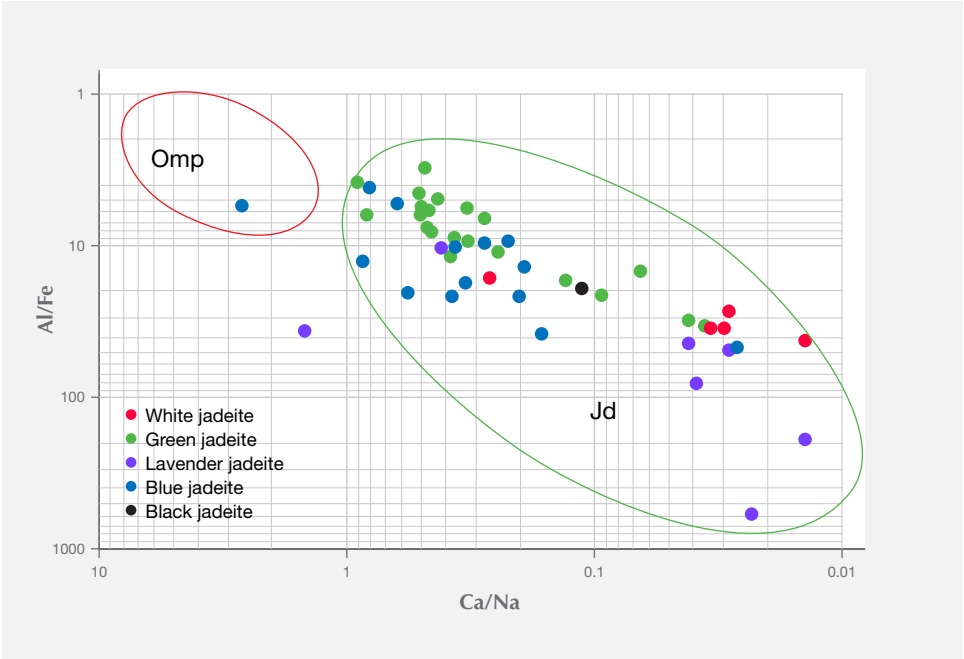

Figure 16. Chemical fingerprinting of Al/Fe vs. Ca/Na indicates the separation of jadeite (Jd) from omphacite (Omp) jade according to chemical concentration. Although the data plotted here were collected from LA-ICP-MS analysis, this type of diagram can also be adapted to EDXRF or electron microprobe data.

TABLE 1. Electron microprobe analyses of major element compositions of jadeite jade from Japan, Guatemala, and Russia.

	Itoigawa	Itoigawa		Itoigawa		Itoigawa		Itoigawa		Itoigawa	
	K-IT-JP-14 (5 spots) White	K-IT-JP-14 (12 spots) Green		K-IT-JP-11 (3 spots) Green		K-IT-JP-12 (3 spots) Green		K-IT-JP-13 (3 spots) Green		K-IT-JP-25 (6 spots) Lavender (Violet)	
Oxides (wt.%)	Averaged	Max X_{Jd}%	Min X_{Jd}%	Max X_{Jd}%	Min X_{Jd}%	Max X_{Jd}%	Min X_{Jd}%	Max X_{Jd}%	Min X_{Jd}%	Max X_{Jd}%	Min X_{Jd}%
SiO_2	58.82	60.466	58.95	58.43	57.83	59.25	58.4	59.31	57.11	59.542	59.621
TiO_2	0.03	0	0.02	0.012	0	0	0	0	0.012	0.362	0.325
Al_2O_3	24.3	24.822	24.3	22.38	20.59	21.87	20.83	21.98	21.27	24.518	22.997
Cr_2O_3	0	0.036	0.09	0.16	0.085	0.013	0.01	0.152	0.577	0.083	0.008
FeO	0.44	0.225	0.45	0.561	0.864	0.744	0.744	0.425	0.481	0.105	0.694
MnO	0	0.013	0.01	0.033	0	0.02	0.022	0.007	0.008	0.019	0
MgO	0.12	0.16	0.54	1.8	2.83	1.83	2.78	2.2	2.41	0.064	0.864
CaO	0.26	0.24	0.92	2.7	4.18	3.02	4.15	3.8	5.1	0.644	1.879
Na_2O	15.49	14.113	14.91	13.94	12.77	13.55	13.03	13.22	11.88	14.278	13.31
K_2O	0	0	0	0.01	0	0	0	0	0	0.001	0
NiO	0	0	0	0	0.032	0	0.025	0.022	0.025	0.011	0
Total	**99.46**	**100.075**	**100.2**	**100.025**	**99.181**	**100.296**	**99.992**	**101.116**	**98.873**	**99.627**	**99.895**
Cations (O=6)											
Si	2	2.026	1.991	1.989	1.994	2.009	1.996	1.999	1.975	2.001	2.02
Ti	0.001	0	0	0	0	0	0	0	0	0.008	0.008
Al	0.974	0.98	0.967	0.898	0.837	0.874	0.839	0.872	0.867	0.991	0.919
Cr	0	0.001	0.003	0.004	0.002	0	0	0.004	0.016	0	0
Fe*	0.013	0.006	0.013	0.016	0.024	0.02	0.021	0.012	0.014	0.002	0.019
Mn	0	0	0	0.001	0	0.001	0.001	0	0	0	0
Mg	0.006	0.008	0.027	0.091	0.145	0.093	0.142	0.11	0.124	0.001	0.04
Ca	0.009	0.009	0.033	0.098	0.154	0.11	0.152	0.137	0.189	0.023	0.068
Na	1.021	0.917	0.977	0.92	0.854	0.891	0.864	0.863	0.796	0.932	0.875
K	0	0	0	0	0	0	0	0	0	0.003	0.008
Ni	0	0	0	0	0.001	0	0.001	0.001	0	0	0
Total	**4.023**	**3.947**	**4.012**	**4.019**	**4.013**	**3.999**	**4.016**	**3.997**	**3.982**	**3.961**	**3.965**
End members (mol%) after Morimoto et al. (1988)											
X_{Jd}	98	98.7	95.5	88.5	82.6	88.9	83.3	86.6	82.4	98.7	93.3
$X_{(Ae+Ko)}$	1.2	0.1	1.5	2	2.3	1.7	2.1	0.4	1.6	0	0
X_{Quad}	0.8	1.2	3	9.5	15.1	10.3	14.6	13	16	1.3	6.7

high-pressure assemblage, which may contain the same accessory phases (amphibole, feldspar, and lawsonite) as jadeite from Itoigawa-Omi.

Blue Jadeite. The six blue samples from Itoigawa and the two violetish blue specimens from Wakasa had significantly high TiO_2, with maximum values of 0.649 and 0.745 wt.%, respectively. These corresponded with the intense blue area. The CaO contents were slightly higher in the light blue to blue areas (0.6% to 1.4 wt.%) than in the white areas. Violetish blue and blue areas revealed the highest concentration of Ti measured in Japanese jadeite (up to 4520 ppmw in blue jadeite from Itoigawa, and up to 3636 ppmw in violetish blue jadeite from Wakasa), as well as enriched Fe (up to 11,900 ppmw). Most of the REE contents were higher than in lavender jadeite.

Chondrite-Normalized REE and Primitive Mantle–Normalized Heavy Trace Element Pattern. To compare trace element compositions in different colors of Japanese jadeite, we studied their chondrite-normalized REE patterns and primitive mantle–normalized trace element patterns. Figures 17 and 18 show the averaged REE and heavy trace element data of white, black, green, lavender, and blue jadeite from Itoigawa-Omi, along with two violetish blue specimens from Wakasa. The REEs in Japanese jadeite tended to be more abundant in lavender, violetish blue, and blue specimens than in green, white, and black jadeite. In all colors, the light rare earth element (LREE: La, Ce, Nd, and Sm) contents tended to be higher than the heavy rare earth element (HREE: Eu, Gd, Dy, Y, Er, Yb, and Lu) contents. From this chondrite-normalized REE pattern, the lavender, violetish blue, and blue

Itoigawa		Wakasa		Matuaga		Matuaga		Polar Urals	
K-IT-JP-16 (6 spots) Blue		W-TO-JP-02 (6 spots) Violetish blue		M-GUA-03 (5 spots) Lavender (Violet)		M-GUA-02 (8 spots) Grayish green		PU-RUS-03 (11 spots) Green	
Max X_{Jd}%	Min X_{Jd}%	Max X_{Jd}%	Min X_{Jd}%	Max X_{Jd}%	Min X_{Jd}%	Max X_{Jd}%	Min X_{Jd}%	Max X_{Jd}%	Min X_{Jd}%
60.728	59.768	58.041	58.899	61.733	58.149	60.898	59.518	58.789	58.518
0.106	0.649	0.745	0.173	0.04	0.07	0.28	0.05	0.073	0.106
24.872	22.995	22.867	24.731	22.927	24.614	23.672	19.48	20.482	19.517
0.001	0.052	0	0.048	0	0.005	0	0	0.385	0.139
0.214	0.445	0.615	0.6	0	0.187	0.836	1.891	0.725	0.761
0.026	0	0.051	0.039	0	0.006	0.039	0.013	0.071	0.019
0.478	1.105	1.532	0.225	0.057	0.015	0.314	2.354	2.639	3.441
0.629	1.436	2.24	0.659	0.108	0.231	0.634	3.718	3.786	4.801
14.113	13.767	13.02	13.43	13.097	14.022	14.595	11.876	12.515	11.347
0.027	0.011	0	0.036	0.149	0.01	0	0	0.01	0.032
0.024	0.006	0	0	0	0.007	0.039	0.012	0.088	0.03
101.218	**100.234**	**99.111**	**98.84**	**98.108**	**97.316**	**101.307**	**98.912**	**99.563**	**98.711**
2.019	2.034	1.997	2.004	2.09	2.005	2.031	2.071	2.038	2.05
0.002	0.006	0.019	0.004	0.001	0.002	0.007	0.001	0.002	0.003
0.974	0.916	0.927	0.992	0.915	1	0.93	0.799	0.837	0.806
0	0.001	0	0.001	0	0.001	0	0	0.011	0.004
0.006	0.013	0.018	0.017	0	0.005	0.023	0.057	0.021	0.022
0.001	0	0.001	0.001	0	0	0.001	0	0.002	0.001
0.024	0.056	0.078	0.011	0.003	0.001	0.016	0.122	0.136	0.18
0.022	0.052	0.083	0.024	0.004	0.009	0.023	0.139	0.141	0.18
0.909	0.902	0.869	0.886	0.86	0.938	0.944	0.801	0.841	0.771
0.001	0	0	0.002	0.006	0	0	0	0	0.001
0.001	0	0	0	0	0	0.001	0	0.002	0.001
3.958	**3.981**	**3.993**	**3.944**	**3.879**	**3.962**	**3.976**	**3.99**	**4.031**	**4.019**
97.4	93.7	91.2	97.3	99.6	99.2	96.1	83.4	84	80.5
0	1	0	0.1	0	0.1	1.4	0.3	1.1	0.4
2.6	6.2	8.8	2.6	0.4	0.7	2.5	16.3	14.9	19.1

jadeite from Japan can be characterized by a high LREE/HREE ratio and a low Eu concentration relative to other REE (again, see figure 17).

Interestingly, the primitive mantle–normalized trace element patterns of all colors of Japanese jadeite showed strong positive anomalies of the large-ion lithophile elements (LILE) Sr and Ba, as well as the high field strength elements (HFSE) Zr and Nb. Green jadeite REE patterns were more depleted, but much higher than white and black jadeite, with strong positive anomalies of Sr, Zr, and Hf. This result is consistent with the conclusion by Morishita et al. (2007) that the fluid related to the formation of Itoigawa-Omi jadeite in the subduction zone was uniquely enriched in both LILE[1] and HFSE[2] brought in by the fluids in the subduction zone, and that these elements were recycled into serpentinized peridotites.

By comparison, Russian white and green jadeite revealed the highest REE and heavy trace element values in this study. Green jadeite from Japan and Myanmar showed a very close overlap, whereas the REE and heavy element contents for white samples from Myanmar were very depleted and had the lowest value.

In lavender and blue samples, Guatemalan jadeite

[1]LILE refers to lithophile trace elements (K, Rb, Cs, Sr, Ba, Pb, and Eu), which have an ionic radius to charge ratio that is greater than those of Ca^{2+} and Na^{+}, the largest cations common to rock-forming minerals.

[2]HFSE refers to high field strength elements (Ti, Zr, Hf, Nb, and Ta), which do not have a large ionic radius. Because of their high charge and the consequent difficulty in achieving a charge balance, they are typically incompatible.

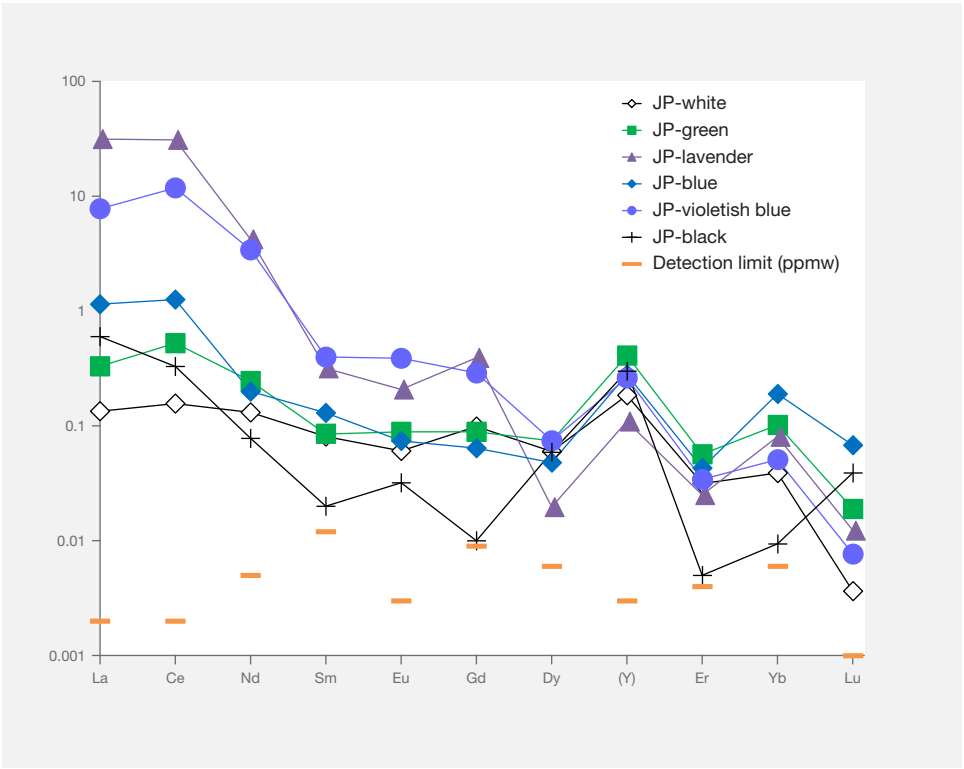

Figure 17. Chondrite-normalized rare earth element (REE) patterns are shown for each color of Japanese jadeite.

was characterized by the highest REE and heavy trace element concentrations. Japanese material showed a lower value but could be separated from Burmese lavender jadeite based on the chondrite-normalized and primitive mantle–normalized patterns.

CONCLUSIONS

Japanese jadeite from the Itoigawa-Omi region is characterized by mixtures of white with green and other colors such as lavender, blue, and black. Although jadeite mining has been prohibited there since 1954, small pebbles can be found along the rivers or estuaries. In this study, a large number of samples from Itoigawa-Omi and Wakasa were analyzed to characterize the chromophores, optical absorption features, and quantitative chemical composition of major and trace elements in each color variety. This gemological, petrographic, and chemical study also included Burmese, Guatemalan, and Russian jadeite samples for comparison. The results are summarized below.

1. Jadeite boulders and pebbles from Itoigawa-Omi tended to have rounded corners from fluvial erosion and showed a glittering whitish surface, but the rough rock did not show a weathered brown skin. The Japanese jadeite was mainly white, with unevenly distributed pale green to green and lavender to blue color.
2. Petrographic observations showed that Japanese jadeite was composed of aggregates of long, semi-euhedral prismatic crystals and granular single crystals, which combined to produce a prismatic-granular crystalloblastic texture. Pectolite, prehnite, and analcime were often present in folding, faults, and veinlets, while the minor component minerals vesuvianite and titanite were found in the matrix.
3. Quantitative analysis by electron microprobe showed that the white jadeite was close to pure jadeite ($X_{Jd} = 98$). Green jadeite was in the range of $X_{Jd} = 98–82$ and $X_{Aeg} = 2–8$, and the chromophores Fe and Cr were responsible for the green color. Lavender color was produced by a combination of higher Ti and Fe and lower Mn. In blue jadeite, the Ti^{4+}-Fe^{2+} charge-transfer played a significant role in coloration.
4. LA-ICP-MS analysis detected 19 minor and trace elements. The chondrite-normalized rare earth element and primitive mantle–normalized heavy trace element patterns of all colored jadeite showed higher light REE than heavy REE, along with positive large-ion lithophile el-

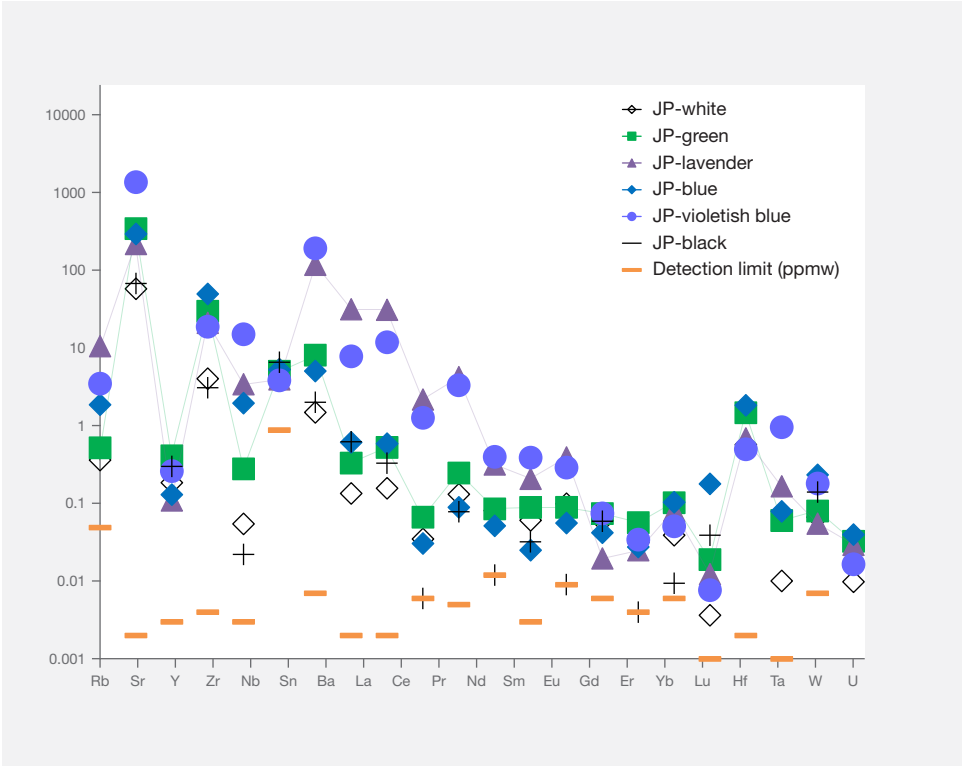

Figure 18. Primitive mantle–normalized heavy trace element patterns are shown for each color of Japanese jadeite.

ements and high field strength element anomalies. Lavender and blue (including violetish blue) jadeite had dominant REE compared to green jadeite, whereas white and black jadeite had the lowest REE contents.

Our studies confirmed that green jadeite from Itoigawa, Myanmar, and Russia have similar gemological properties such as RI and SG and absorption spectra of Cr and Fe, while Guatemalan grayish green jadeite does not contain Cr. Lavender jadeite from Japan and Guatemala showed similar color, caused by high Ti and Fe and low Mn. Investigation of thin sections revealed that Burmese jadeite contains kosmochlor, amphibole, albite, nepheline, and vesuvianite. Russian jade has the very common mineral magnetite in matrix and analcime in veinlets. Guatemalan jadeite was characterized by grossular garnet, albite, rutile, and other minerals. While Guatemalan jadeite contained abundant REEs and heavy trace elements, Burmese jade had much lower values. Japanese jadeite shows characteristic trace elements and matrix inclusion varieties that may be useful in establishing the precise country of origin.

ABOUT THE AUTHORS

Dr. Abduriyim is president of Tokyo Gem Science, LLC and director of GSTV Gemological Laboratory. He is a former senior manager and senior scientist of GIA's laboratory in Tokyo. Dr. Saruwatari and Dr. Katsurada are scientists and staff gemologists at GIA's laboratory in Tokyo.

ACKNOWLEDGMENTS

The authors thank Nobuyuki Tsurumi (The Jade Ore Museum/Hisui Gensekikan, Tokyo), Minoru Kameyama (Miyuki Co., Tokyo), and Prof. Miyajima (Fossa Magna Museum, Itoigawa) for information and specimens that made this study possible. We sincerely thank Dr. Mikouchi, associate professor at the University of Tokyo, and Prof. Ogasawara and Dr. Sakamaki at Waseda University for providing EPMA testing. We are also grateful to GIA colleagues Dr. Shoko Odake and Dr. Supharart Sangsawong, who assisted with data collection. The authors wish to thank Dr. F. Lin Sutherland, a former curator and research scientist at the Australian Museum in Sydney, for his critique of the manuscript.

REFERENCES

Barnes G.L. (1999) *The Rise of Civilization in East Asia: The Archaeology of China, Korea and Japan*. Thames and Hudson, New York.

Burns R.G. (1981) Intervalence transitions in mixed-valence minerals of iron and titanium. *Annual Review of Earth and Planetary Sciences*, Vol. 9, No. 1, pp. 345–383, http://dx.doi.org/10.1146/annurev.ea.09.050181.002021

Chihara K. (1971) Mineralogy and paragenesis of jadeites from the Omi-Kotaki area, Central Japan. *Mineralogical Society of Japan, Special Paper*, No. 1, pp. 147–156.

Chihara K. (1991) Jade in Japan. In R. Keverne, Ed., *Jade*. Van Nostrand Reinhold, New York, pp. 216–217.

Essene E.J. (1967) An occurrence of cymrite in the Franciscan formation, California. *American Mineralogist*, Vol. 52, pp. 1885–1890.

Ferguson J., Fielding P.E. (1971) The origins of the colours of yellow, green, and blue sapphires. *Chemical Physics Letters*, Vol. 10, No. 3, pp. 262–265, http://dx.doi.org/10.1016/0009-2614(71)80282-8

Foshag W.F., Leslie R. (1955) Jadeite from Manzanal, Guatemala. *American Antiquity*, Vol. 21, No. 1, pp. 81–83, http://dx.doi.org/10.2307/276111

Fukuyama M., Ogasawara M., Horie K., Lee D.C. (2013) Genesis of jadeite-quartz rocks in the Yorii area of the Kanto Mountains, Japan. *Journal of Asian Earth Sciences*, Vol. 63, pp. 206–217, http://dx.doi.org/10.1016/j.jseaes.2012.10.031

Harlow G.E., Olds E.P. (1987) Observations on terrestrial ureyite and ureyitic pyroxene. *American Mineralogist*, Vol. 72, pp. 126–136.

Harlow G.E., Sorensen S.S. (2005) Jade (nephrite and jadeitite) and serpentinite: Metasomatic connections. *International Geology Review*, Vol. 47, No. 2, pp. 113–146, http://dx.doi.org/10.2747/0020-6814.47.2.113

Kanmera K., Hashimoto M., Matsuda T. (1980) *Geology of Japan*. Vol. 15 of Iwanami Koza Chikyukagaku series. Iwanami Shoten, Tokyo, 387 pp. (in Japanese).

Kawano Y. (1939) A new occurrence of jade (jadeite) in Japan and its chemical properties. *Journal of the Japanese Association of Mineralogists, Petrologies and Economic Geologists*, No. 22, pp. 195–201 (in Japanese).

Kunugiza K., Nakamura E., Miyajima H., Goto A., Kobayashi K. (2002) Formation of jadeite-natrolite rocks in the Itoigawa-Ohmi area of the Hida marginal belt inferred from U-Pb-zircon dating. Abstract of annual meeting of the Japanese Association of Mineralogists, Petrologists and Economic Geologists in 2002, GP20 (in Japanese)

Lu R. (2012) Color origin of lavender jadeite: An alternative approach. *G&G*, Vol. 48, No. 4, pp. 273–283, http://dx.doi.org/10.5741/GEMS.48.4.273

Miyajima H., Matsubara S., Miyawaki R., Ito K. (1999) Itoigawaite, a new mineral, the Sr analogue of lawsonite, in jadeite from the Itoigawa-Ohmi district, central Japan. *Mineralogical Magazine*, Vol. 63, No. 6, pp. 909–916, http://dx.doi.org/10.1180/002646199548899

Miyajima H., Matsubara S., Miyawaki R., Yokoyama K., Hirokawa K. (2001) Rengeite, $Sr_4ZrTi_4Si_4O_{22}$, a new mineral, the Sr-Zr analogue of perrierite from Itoigawa-Ohmi district, Niigata Prefecture, central Japan. *Mineralogical Magazine*, Vol. 65, No. 1, pp. 111–120, http://dx.doi.org/10.1180/002646101550163

Miyajima H., Miyawaki R., Ito K. (2002) Matsubaraite, $Sr_4Ti_5(Si_2O_7)_2O_8$, a new mineral, the Sr-Ti analogue of perrierite in jadeitite from the Itoigawa-Ohmi district, Niigata Prefecture, Japan. *European Journal of Mineralogy*, Vol. 14, No. 6, pp. 1119–1128, http://dx.doi.org/10.1127/0935-1221/2002/0014-1119

Miyawaki R. (2004) Main minerals of jadeite jade. *Gemmology*, Vol. 35, No. 420, pp. 14–15 (in Japanese).

Miyazoe T., Nishiyama T., Uyeta K., Miyazaki K., Mori Y. (2009) Coexistence of pyroxenes jadeite, omphacite, and diopside-hedenbergite rock from a serpentinite mélange in the Kurosegawa zone of central Kyushu, Japan. *American Mineralogist*, Vol. 94, No. 1, pp. 34–40.

Morimoto N., Fabries J., Ferguson A.K., Ginzburg I.V., Ross M., Seifert F.A, Zussman J., Aoki K., Gottardi G. (1988) Nomenclature of pyroxenes. *American Mineralogist*, Vol. 73, pp. 1123–1133.

Morishita T. (2005) Occurrence and chemical composition of barian feldspar in a jadeitite from the Itoigawa-Ohmi district in the Renge high-P/T-type metamorphic belt, Japan. *Mineralogical Magazine*, Vol. 69, No. 1, pp. 39–51, http://dx.doi.org/10.1180/0026461056910237

Morishita T., Arai S., Ishida Y. (2007) Trace element compositions of jadeite (+omphacite) in jadeitites from the Itoigawa-Ohmi district, Japan: Implications for fluid processes in subduction zones. *Island Arc*, Vol. 16, No. 1, pp. 40–56, http://dx.doi.org/10.1111/j.1440-1738.2007.00557.x

Nakamizu M., Okada M., Yamazaki T., Komatsu M. (1989) Metamorphic rocks in the Omi-Renge serpentinite mélange, Hida Marginal Tectonic Belt, Central Japan. *Memoirs of the Geological Society of Japan*, Vol. 33, pp. 21–35 (in Japanese with English abstract).

Nishimura Y. (1998) Geotectonic subdivision and areal extent of the Sangun belt, inner zone of southwest Japan. *Journal of Metamorphic Geology*, Vol. 16, No. 1, pp. 129–140, http://dx.doi.org/10.1111/j.1525-1314.1998.00059.x

Oberhänsli R., Bousquet R., Moinzadeh H., Moazzen M., Arvin M. (2007) The field of stability of blue jadeite: A new occurrence of jadeitite at Sorkhan, Iran, as a case study. *Canadian Mineralogist*, Vol. 45, No. 6, pp. 1501–1509, https://doi.org/10.3749/canmin.45.6.1501

Ohmori K. (1939) Optical properties of jade (jadeite) newly occurred in Japan. *Journal of the Japanese Association of Mineralogists, Petrologists and Economic Geologists*, No. 22, pp. 201–212 (in Japanese).

Rossman G.R. (1974) Lavender jade. The optical spectrum of Fe^{3+} and Fe^{2+}→Fe^{3+} intervalence charge transfer in jadeite from Myanmar. *American Mineralogist*, No. 59, pp. 868–870.

Shibata K., Nozawa T. (1968) K-Ar age of Omi schist, Hida Mountains, Japan. *Bulletin of the Geological Survey of Japan*, No. 19, pp. 243–246.

Shinno I., Oba T. (1992) Absorption and photo-luminescence spectra of Ti^{3+} and Fe^{3+} in jadeites. *Mineralogical Journal*, Vol. 16, No. 7, pp. 378–386, http://dx.doi.org/10.2465/minerj.16.378

Shoji T., Kobayashi S. (1988) Fluid inclusions found in jadeite and stronalsite, and a comment on the jadeite-analcime boundary. *Journal of Mineralogy, Petrology and Economic Geology*, Vol. 83, No. 1, pp. 1–8, http://dx.doi.org/10.2465/ganko.83.1

Sorensen S.S., Harlow G.E., Rumble D. III. (2003) SIMS oxygen isotope analyses of jadeitite: trace element correlations, fluid compositions, and temperature estimates. *Geological Society of America Abstract with Program*, Vol. 35, No. 6, pp. 90–97.

Takayama M. (1986) Mode of occurrence and significance of jadeite in the Kamuikotan metamorphic rocks, Hokkaido, Japan. *Journal of Metamorphic Geology*, Vol. 4, No. 4, pp. 445–454, http://dx.doi.org/10.1111/j.1525-1314.1986.tb00363.x

Taube K.A. (2004) Olmec art at Dumbarton Oaks. Dumbarton Oaks Research Library and Collection, Washington, D.C.

Tsujimori T. (2002) Prograde and retrograde P-T paths of the Late Paleozoic glaucophane eclogite from the Renge metamorphic belt, Hida Mountains, southwestern Japan. *International Geology Review*, Vol. 44, No. 9, pp. 797–818, http://dx.doi.org/10.2747/0020-6814.44.9.797

Tsutsumi Y., Yokoyama K., Miyawaki R., Matsubara S., Terada K.,

Hidaka H. (2010) Ages of zircons in jadeitite and jadeite-bearing rocks of Japanese islands. *Bulletin of the National Museum of Nature and Science*, Vol. 36, pp. 19–30.
Umehara S. (1971) *Japan Ancient Jade Memorandum*. Yoshikawa Hirobunkan, Tokyo (in Japanese), 354 pp.
Yokoyama K., Sameshima T. (1982) Miscibility gap between jadeite and omphacite. *Mineralogical Journal*, Vol. 11, pp. 53–61, http://dx.doi.org/10.2465/minerj.11.53

ADDITIONAL READING

Abduriyim A., Kitawaki H. (2006) Determination of the origin of blue sapphire using laser ablation inductively coupled plasma mass spectrometry (LA-ICP-MS). *The Journal of Gemmology*, Vol. 30, No. 1/2, pp. 23–42.
Abduriyim A., Kitawaki H., Furuya M., Schwarz D. (2006) "Paraiba"-type copper-bearing tourmaline from Brazil, Nigeria, and Mozambique: Chemical fingerprinting by LA-ICP-MS. *G&G*, Vol. 42, No. 1, pp. 4–21, http://dx.doi.org/10.5741/GEMS.42.1.4
Blodgett T., Shen A.H. (2011) Application of discrimination analysis in gemology: Country-of-origin separation in colored stones and distinguishing HPHT-treated diamonds. *G&G*, Vol. 47, No. 2, p. 145.
Breeding C.M., Shen A.H. (2010) LA-ICP-MS analysis as a tool for separating natural and synthetic malachite. *News from Research*, Oct. 11, http://www.gia.edu/gia-news-research-nr101410
Fisher R.A. (1936) The use of multiple measurements in taxonomic problems. *Annals of Eugenics*, Vol. 7, No. 2, pp. 179–188, http://dx.doi.org/10.1111/j.1469-1809.1936.tb02137.x.
Harlow G.E., Shi G.H. (2011) An LA-ICP-MS study of lavender jadeite from Myanmar, Guatemala, and Japan. *G&G*, Vol. 47, No. 2, pp. 116–117.
Iwao S. (1953) Albitite and associated jadeite rock from Kotaki district, Japan: A study in ceramic raw material. *Bulletin of the Geological Survey of Japan*. No. 153, pp. 1–26.
Kobayashi S., Miyake H., Shoji T. (1986) A jadeite rock from Oosa-cho, Okayama Prefecture, southwestern Japan. *Mineralogical Journal*, Vol. 13, No. 6, pp. 314–327, http://dx.doi.org/10.2465/minerj.13.314
Luo Z.M, Yang M.X., Shen A.H. (2015) Origin determination of dolomite-related white nephrite through IB-LDA. *G&G*, Vol. 51, No. 3, pp. 300–311, http://dx.doi.org/10.5741/GEMS.51.3.300
McDonough W.F., Sun S.S. (1995) The composition of the Earth. *Chemical Geology*, Vol. 120, Nos. 3–4, pp. 223–253, http://dx.doi.org/10.1016/0009-2541(94)00140-4
Miyajima H. (2014) *Story of the Much-Valued Jadeite*. Fossa Magna Museum and Education Committee of Itoigawa, Itoigawa, 96 pp. (in Japanese).
Oba T., Nakagawa Y., Kanayama K., Watanabe T. (1992) Notes on rock-forming minerals in the Joetsu district, Niigata Prefecture, Japan: (5) Lavender jadeite from the Kotaki river. *Bulletin of Joetsu University of Education*, No. 11, pp. 367–375.
Ouyang Q. (2001) Characteristic of violet jadeite jade and its coloration mechanism. *Journal of Gems and Gemmology*, Vol. 3, No. 1, pp. 1–6 (in Chinese).
Rankin A.H., Greenwood J., Hargreaves D. (2003) Chemical fingerprinting of some East African gem rubies by laser ablation-ICP-MS. *The Journal of Gemmology*, Vol. 28, No. 8, pp. 473–482.
Saeseaw S., Pardieu V., Sangsawong S. (2014) Three-phase inclusions in emeralds and their impact on origin determination. *G&G*, Vol. 50, No. 2, pp. 114–132, http://dx.doi.org/10.5741/GEMS.50.2.114
Saminpanya S., Manning D.A.C., Droop G.T.R., Henderson C.M.B. (2003) Trace elements in Thai gem corundums. *The Journal of Gemmology*, Vol. 28, No. 7, pp. 399–415.
Shen A.H., Blodgett T., Shigley J.E. (2013) Country-of-origin determination of modern gem peridots from LA-ICP-MS trace-elements chemistry and linear discriminant analysis (LDA). *Geological Society of America Abstracts with Programs*, Vol. 45, No. 7, p. 525.
Sutherland F.L., Schwarz D., Jobbins E.A., Coenraads R.R., Webb G. (1998) Distinctive gem corundum suites from discrete basalt fields: A comparative study of Barrington, Australia, and West Pailin, Cambodia, gemfields. *The Journal of Gemmology*, Vol. 26, No. 2, pp. 65–85.